Dendrochronologia 63 (2020) 125755

Contents lists available at ScienceDirect

Dendrochronologia

journal homepage: www.elsevier.com/locate/dendro

ORIGINAL ARTICLE

Does signal-free detrending increase chronology coherence in large tree-ring networks?

M.Y. McPartland [a,*], S. St. George [a], Gregory T. Pederson [b], Kevin J. Anchukaitis [c]

[a] Department of Geography, Environment & Society, University of Minnesota, United States
[b] U.S. Geological Survey, Northern Rocky Mountain Science Center, Bozeman, MT, United States
[c] Laboratory of Tree-Ring Research and School of Geography, Development, and Environment, University of Arizona, Tucson, AZ, United States

ARTICLE INFO

Keywords:
Dendrochronology
Tree-rings
Signal-free detrending
Paleoclimatology

ABSTRACT

Over the past decade, dendrochronologists have increasingly adopted the signal-free detrending (SFD) method to remove age-size trends in tree-ring measurement series, amplify the common stand-wide signal in composite chronologies, and recover medium- to low-frequency patterns that may be inadvertently removed by other detrending approaches. However, since its introduction in 2008, no systematic evaluation of the effects of SFD on tree-ring chronologies has been performed. Here we conduct the first review of SFD in dendrochronology and assess its effects when applied to large tree-ring networks. We analyzed the PAGES North America 2 K database of nearly 300 temperature-sensitive chronologies and the Missouri River database of over 350 chronologies curated for the purpose of reconstructing Missouri River streamflow. Both databases contain multiple versions of each chronology generated by different detrending methods, including those produced with (and without) the signal-free procedure applied. We evaluated (i) whether SFD increases chronology coherence at the site level by boosting the between-tree agreement, (ii) whether SFD increases coherence on a regional basis by making neighboring chronologies more similar to each other, and (iii) whether signal-free chronologies retained more medium- to low-frequency variability than their traditional counterparts. We find that, while SFD increased the strength of common signals in many instances, the effect was not universal and some sites even show a decrease in signal coherence. At regional scales, SFD increases chronology coherence in temperature-sensitive records but had no detectable effect on moisture-sensitive records. Our results demonstrate the importance of evaluating the effects of SFD prior to deploying this method for chronology development and paleoclimate reconstruction.

1. Introduction

Detrending is an essential data processing step in the development of tree-ring chronologies. This practice is intended to remove the geometric age- and size-related growth trend and emphasize the common climate-related variance within a site or region (Fritts, 1976). Functionally, detrending involves transforming raw tree-ring measurements into dimensionless ring-width indices, typically by dividing or subtracting measurements against an idealized estimate of growth trends obtained from a data-adaptive spline, linear regression, or negative exponential curve function (Cook and Kairiukstis, 1990). Although these methods remove the pattern of rapid growth often present at the beginning of tree-ring series, they are imperfect tools because annual ring width represents a complex aggregate of environmental, ecological, and age-related factors (Fritts, 1976; Cook, 1987). This complexity leaves open the question of how much of the low-frequency (decadal-to-centennial-scale) variability that is removed by detrending in any given ring-width series is related to climate or other biological or environmental factors. Low-frequency climate signals can be removed during detrending and many standardization techniques emphasize high-frequency (i.e., interannual to decadal) variability (Briffa et al., 1996; Esper et al., 2002; Cook et al., 1995). In addition, in cases where chronologies consist of many short individual ring-width series, low-frequency climate related signals are not retained due to the problem known as the “segment-length” curse (Cook et al., 1995). In this situation, the growth trend removal from traditional detrending techniques employed on the many short individual series combined with the process of averaging these records into a site chronology removes variability at multi-decadal or greater timescales. Consequently, some unknown amount of climate-related variance is lost during detrending

* Corresponding author.
E-mail address: mcpar046@umn.edu (M.Y. McPartland).

https://doi.org/10.1016/j.dendro.2020.125755
Received 15 May 2020; Received in revised form 8 August 2020; Accepted 27 August 2020
Available online 1 September 2020
1125-7865/

and some non-climatic information is propagated into the resulting ring-width indices (Briffa et al., 1996).

A variety of detrending methods have been developed for the purpose of removing age-growth trends while maximizing the retention of climate signals at medium and low frequencies. For example, regional curve standardization (RCS) develops a stand-wide detrending curve by aligning samples by cambial age in order to approximate a regional growth trend (Helama et al., 2004; Esper et al., 2003; Helama et al., 2017). Bias in final chronologies may result from RCS if all of the trees represented within a chronology do not reflect a single growth curve through time (Briffa and Melvin, 2011; Anchukaitis et al., 2013). The result of biases introduced during detrending is that traditional methods such as RCS, negative exponential curve, or spline fitting may result in "trend distortion", a term used to describe a mismatch between tree-ring indices and climate data (Helama et al., 2004; Melvin, 2004; Melvin and Briffa, 2014a, 2014b, Melvin and Briffa, 2008). Trend distortion can also result from dividing raw measurements by a near-zero growth curve, resulting in artificially inflated estimates of climate, particularly at the modern end of chronologies (Cook and Peters, 1997; D'Arrigo et al., 2008). The discarding or artificial amplification of common low-frequency growth variability related to climate, and/or the introduction of bias due to detrending limits our ability to correctly calibrate tree-ring chronologies against instrumental climate records and reconstruct centennial- and greater-scale climate variability (Briffa and Melvin, 2011; Helama et al., 2017).

Signal-free detrending (SFD) was first introduced by Melvin (2004) as a solution to the problem of trend distortion at medium-frequency (decades to a century) timescales, resulting in a mismatch between climate records and tree-ring chronologies (Melvin, 2004; Melvin and Briffa, 2008). The term "signal-free" refers to the creation of detrending curves that do not contain the common signals shared across the trees in a chronology, and are thus 'free' from common variance and should preserve this signal in the resulting chronology. Unlike other data-adaptive detrending methods, SFD uses an iterative approach to create individual growth curves in which shared variance lost during the initial detrending process is reintroduced into the ring-width index series (Melvin, 2004; Melvin and Briffa, 2008). In its original formulation, SFD was primarily intended to improve the expression of medium-frequency (i.e., decades to one century) variance associated with climate forcing. Because age-growth trends overlap with decadal-scale variance in tree ring chronologies, climate-related signals at medium frequencies are also subject to removal during traditional detrending. The signal-free approach was designed to minimize distortion at these frequencies, thus improving the quality of tree-ring chronologies for use in paleoclimate reconstruction.

In theory, the use of the signal-free approach to detrending should increase the expression of common signals that are present among trees within chronologies as well as between neighboring chronologies with similar environmental limitations on tree growth. Because it is designed to preserve medium-frequency variance, SFD should also increase the expression of multi-decadal to centennial trends attributable to climate forcing of temperature and/or hydroclimate (Briffa et al., 2001; Esper et al., 2002; Cook et al., 2007). Despite widespread use, the efficacy of this method has not been evaluated with respect to its effects on diverse types of chronologies (e.g. moisture versus temperature-sensitive), such as those included in large networks of tree ring datasets. In this study, we reviewed published studies that used SFD in order to gage how this method has been applied by the dendrochronology research community.

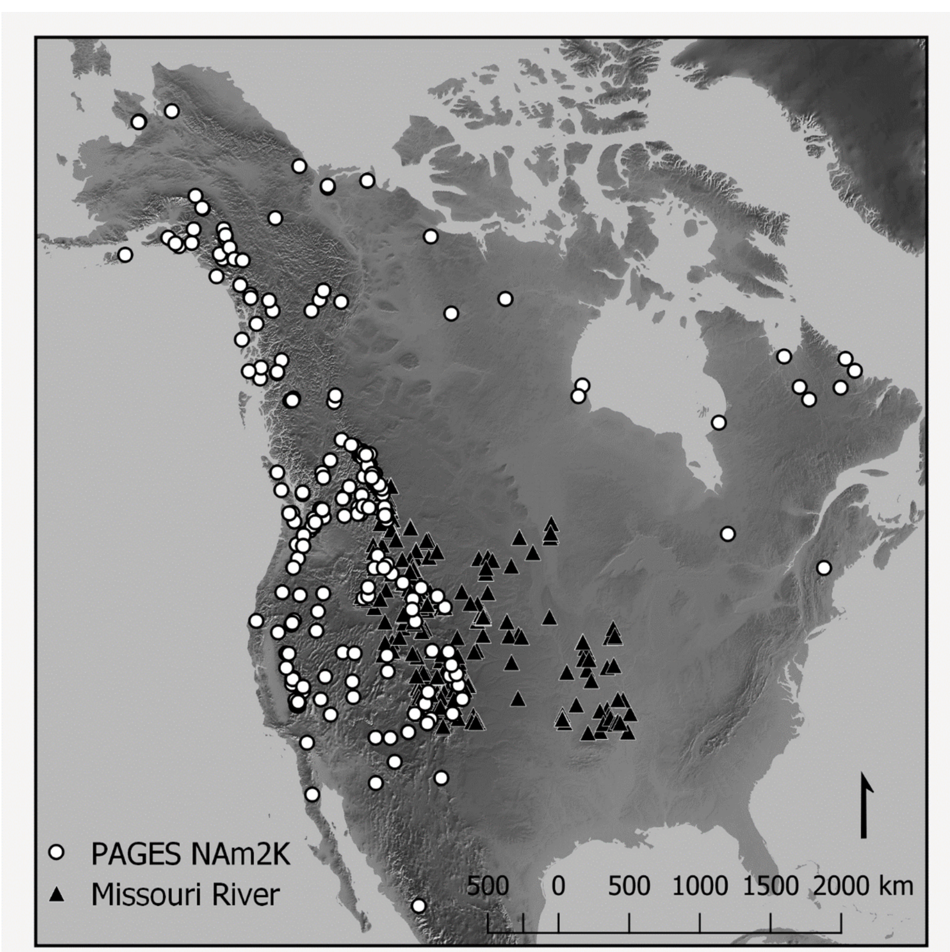

Fig. 1. Map of locations for Past Global Changes (PAGES) North America 2 K and Missouri River Basin site chronologies. Both networks of chronologies were developed for use in paleoclimate reconstruction. The PAGES database (n = 289) contains temperature-sensitive chronologies, most of which were collected at high elevation and far-northern sites. The Missouri River Basin (n = 374) database contains primarily moisture-sensitive chronologies from the eastern Rockies and Great Plains.

We then performed a series of analyses to examine how the signal-free method influences the expression of common signals in large tree-ring networks. We tested whether SFD increased the expression of shared and medium-frequency variance at the site level and on a regional basis in over 600 temperature and moisture-sensitive chronologies from across North America (Fig. 1). Our aim was to examine how SFD changes the expression of common signals in tree-ring chronologies, rather than to test the fidelity of the resulting chronologies to climate records. Our analysis does not address the problem of trend distortion, which would require a comparison of the signals associated with different detrending choices with those present in time series of climate observations. Instead, this review and analysis are intended to highlight how this method has been used in tree-ring research and establish a framework that other dendrochronologists can apply when evaluating the effects of SFD on the development of new tree-ring chronologies.

1.1. Hypotheses

Based on our understanding of how the signal-free process influences tree-ring measurements and chronologies, we hypothesize that *(i) SFD would increase strength of correlations among records at the site level,* representing an increase in the expression of site-wide common signals. On a regional basis, we predict that *(ii) SFD would increase coherence by strengthening correlations between neighboring chronologies,* representing an increase in the strength of regional climate signals. Last, we hypothesize that *(iii) signal-free chronologies would exhibit greater medium (decades to century) and low-frequency (century to millennium) variability compared to traditional versions.*

1.2. A brief overview of signal-free detrending

Signal-free detrending is an iterative, data-adaptive detrending method that can be implemented in conjunction with any of the detrending curves (i.e., negative exponential, cubic smoothing splines, RCS, et cetera) common in tree-ring standardization (Melvin, 2004; Melvin and Briffa, 2008). In a single iteration, individual series are detrended using initial detrending curves representing the expected growth without the influence of climate to create a “tree index” associated with that individual set of measurements. The resulting set of tree indices are averaged together to create a “chronology index” with an associated error term that represents the difference between the stand-wide chronology index and the expected growth in that year:

$$Chronology\ index = \frac{Tree\ index}{Error}$$

From this, the chronology index, or what would be considered “common signal” can be added to or removed by multiplication or division from each series of ring-width measurements in which case:

$$SF\ measurement = \frac{Ring\ width}{Chronology\ index}$$

The mean of the new “signal-free measurement” is then rescaled to the mean of the original set of ring-width measurements, which can then be treated as a raw measurement series. This process is repeated iteratively until the residual chronology indices converge, typically in fewer than six iterations (Melvin, 2004; Melvin and Briffa, 2008). After the indices converge, the residual series are described as “signal-free” because the maximum amount of common signal should have been preserved in the derived tree-ring indices. In theory, the use of the chronology index should have the effect of boosting the commonality of the resulting indices by reintroducing any variance lost during the detrending process. By amplifying common chronology signals, SFD should also have the effect of reducing trend distortion by preserving the real medium- and low-frequency signals present in the tree-ring dataset (Melvin and Briffa, 2008).

2. Methods

2.1. Literature review of SFD use in dendrochronology

The RCSigFree and CRUST programs, which are used to perform signal-free detrending, are available for use by the dendrochronology research community in the software repository at the Lamont-Doherty Earth Observatory Tree-Ring Laboratory (Melvin and Briffa, 2014a (1, 2), Cook et al., 2020 https://www.ldeo.columbia.edu/tree-ring-laboratory/resources/software). To understand how SFD has been used by dendrochronologists we reviewed over 300 citations to Melvin and Briffa (2008) obtained from Google Scholar. If the authors applied this approach in their paper, we recorded the site, species, tree-ring parameter (i.e., tree-ring width, maximum latewood density, etc.), and the climate target (i.e., temperature, rainfall, streamflow, etc.), and curve fitting method. Finally, we noted the rationale stated by the authors for their choice of SFD. Our final literature review included 125 unique studies (See Supplemental Materials for our complete list of articles).

2.2. Testing the effects of SFD on large networks of tree-ring chronologies

We tested the effects of SFD on common chronology signals in two large networks of tree-ring datasets from across North America, developed for use in paleoclimate reconstruction (Fig. 1, Table S1). We analyzed over six hundred temperature and moisture sensitive chronologies to determine the effects of SFD on correlation strength among series within chronologies (i.e., rbar), and between neighboring chronologies on a regional basis. The first network is a set of 298 tree-ring measurement sets from North America curated by the Past Global Changes (PAGES) 2k initiative (PAGES, 2013, 2017). The objective of the PAGES2k effort is to build a community-sourced database of temperature-sensitive proxies, so this compilation only includes tree-ring records (ring width and maximum latewood density, MXD) that are positively and significantly correlated with local temperature observations. Most records within the PAGES North American 2k network (NAM2k) are derived from high-latitude or high-elevation forests in the western Cordillera, Alaska, or northern Canada where summer temperature is the primary climate factor that limits tree growth (St. George, 2014).

The second tree-ring network was developed to support paleohydrological reconstructions for the Missouri River basin (MRB, Martin et al., 2019). This set includes 374 chronologies from the central United States and southern Canada (Fig. 1, Table S1). This network includes chronologies that are reflect variability in streamflow, and therefore it has a variety of different climate sensitivities represented within it including summer temperature, summer precipitation, and winter snowpack (Cook et al., 2007; Woodhouse and Lukas, 2006; Wise, 2010; Pederson et al., 2011; Martin et al., 2019). For every record within the NAM2k and Missouri networks, there are multiple versions of the corresponding chronology, each produced by applying a different detrending method to the same raw tree-ring measurements.

In our analysis, we selected two specific chronology versions that were present in both databases. The first version is derived from a traditional detrending method based on age-dependent spline fitting (Cook and Peters, 1997; Melvin, 2004). The second version had also initially been detrended with age-dependent spline fitting, and then had the iterative signal-free procedure applied in addition (Melvin, 2004; Melvin and Briffa, 2008). In the Missouri River dataset, the initial chronology was generated after detrending each measurement series with an age-dependent spline of unconstrained slope with initial stiffness set to 20-years without variance stabilization. In the NAM2k network, the initial detrending used an age-dependent spline with an initial stiffness or 50-years and a slope constrained to be zero or negative with no variance stabilization.

2.3. Data processing and standardization

Both networks containing the traditional and signal-free chronology versions were subjected to the same screening processes prior to analysis. First, we limited the length of each chronology to the time period from CE 1001-2000, such that no series extended earlier or later than this common period. This step shortened chronologies that started prior to the year 1001, but made no changes to records that began more recently than 1001. Second, we truncated each chronology at the furthest year in the past when the expressed population signal (EPS) dipped below 0.85. This step was applied to ensure a sufficient number of trees were available in each year to produce a reliable estimate of the chronology mean. For chronologies that had a sufficient sample density across the 1000–2000 CE period, no changes were made during this step. All analyses were performed in the R computing environment (R Core Team, 2019).

2.4. Testing the effects of signal-free detrending on stand-level coherence

To determine whether signal-free detrending increases coherence among trees at the site level we analyzed the change in r-bar from the traditional to the signal-free version of each network. R-bar is a traditional statistic in dendrochronology that represents the average correlation among cores within a single tree for a given calendar year (Wigley et al., 1984). We also investigated whether SFD increased the number of years represented in each chronology prior to the 0.85 EPS cutoff. Given that SFD is designed to increase the expression of shared signals within a chronology, we predicted that the signal-free version of each chronology would have a higher r-bar than its traditional chronology counterpart. We also anticipated that SFD would increase the EPS of the resulting chronology, which in turn would cause the signal-free chronologies to extend back further in time compared to the traditional version. To assess statistical significance of change in r-bar, we applied paired Wilcoxon signed-rank tests on Fisher-transformed correlation coefficients (i.e. z-scores) to the two sets of chronology r-bar values resulting from the different detrending methods (Gotelli and Ellison, 2013).

2.5. Analysis of change in chronology coherence at regional scales

Similar to our analysis of change in stand-level coherence, we tested whether SFD increases the similarity between neighboring chronologies. We defined neighboring chronologies as those located at sites within twenty-five kilometers of each other. For each pair, we examined the change in the Pearson correlation coefficient from the traditional to the signal-free version of the chronology. We performed this analysis on smoothed versions of each chronology that we processed using a series of cubic smoothing splines. We used ten, thirty, fifty, and one hundred-year splines with 50 % frequency responses, which means half of the variance at the specified wavelength (i.e., number of years) was retained in the final series. We analyzed the change in correlation between neighbors for the full overlapping portion of the series for the original and smoothed versions of each pair of chronologies. Because SFD is intended to amplify common climate signals, we predicted a significant increase in the correlation between neighboring chronologies would be evident. Because SFD should perform better in retaining lower-frequency variability, we further predicted this effect would be more pronounced in the smoothed version of the analysis. To assess statistical significance of changes in the strength of correlations between sites we performed Wilcoxon signed-rank tests on Fisher-transformed correlation coefficients (i.e. z-scores) for each neighboring pair (Gotelli and Ellison, 2013).

2.6. Determining whether SFD increases variance present at multi-decadal to centennial timescales

We tested whether SFD increases variance present in chronologies at decadal and greater timescales through two separate approaches. First, we computed the power spectrum for each version of the chronologies represented in both networks, and then examined the difference between results obtained from the traditional and SFD versions. For this analysis, we applied spectral analysis on the chronology periodograms, which were smoothed using a Daniell filter with a span length of 2 (Priestley, 1981; Shumway and Stoffer, 2017).

In order to determine how SFD changed the percentage of variance retained at certain wavelengths, we calculated the variance of unsmoothed, ten-year, thirty-year, fifty-year, and one-hundred year smoothed chronologies, and then examined the different in variance present between the traditional and signal-free versions. We predicted that SFD would increase the amount of variance retained at multi-decadal to centennial timescales. The final analysis we performed only on the PAGES network because of its uniform climate sensitivity to summer temperature. Here we averaged all of the traditional and SFD versions of the mean chronology series together and plotted the difference between the traditional and SFD versions at each year from 1001−2000. This step was done to determine the total differences in long-term trends across the two networks.

3. Results

3.1. Literature review

The results of our literature review indicate that SFD has become increasingly common in recent years. In our sample of 125 studies, nearly 90 of them had been published since 2016. We also found that SFD has been applied in wide variety of contexts. Tree-ring parameters were not limited to total ring width and wood density, but also included blue intensity (Deng et al., 2014; Fuentes et al., 2017), wood anatomical features such as microfibral angle and cell wall thickness (Drew et al., 2013; Allen et al., 2017a, b), stable isotope concentrations (Helama et al., 2018), and wood mercury content (Clackett et al., 2018). Around half of the studies that we reviewed used SFD in some type of temperature reconstruction. Approximately one quarter of all studies used SFD to reconstruct precipitation or soil moisture, or to link growth with modes of hydroclimate variability (Cook et al., 2018; Fuentes et al., 2019). Notably, SFD has been integral to the development of all of the major continental-scale drought reconstructions of the Palmer Drought Severity Index (Cook et al., 2013; Palmer et al., 2015; Stahle et al., 2016). The remaining quarter of studies applied SFD to a variety of paleoclimatological analyses such as streamflow reconstructions (Cook et al., 2013; Allen et al., 2017a,b, Maxwell et al., 2017) or in dendroecological applications such as analysis of tree growth rates (Cahoon et al., 2018; Wang et al., 2018, 2019).

Because the signal-free procedure can be applied in conjunction with any type of initial detrending curve, researchers have used SFD with several of the different detrending methods typically used in dendrochronology. Approximately half of the studies reported using some type of data-adaptive spline function as their initial detrending method, such as age-dependent or 2/3rds splines. Over a quarter of the studies used negative exponential or linear curves. Around twenty studies reported using RCS, and the remaining studies reported a variety of different approaches including the Friedman's Super Smoother (Friedman, 1984; Allen et al., 2013, 2015) and Hugershoff curve (Cerrato et al., 2019).

By far the most common reason stated for choosing SFD was to mitigate or reduce trend distortion, followed by a desire to increase the common signal or preserve medium- to low-frequency variability. Very few studies reported having tested multiple approaches before choosing SFD for their final chronology development (e.g. Pederson et al., 2012; Anchukaitis et al., 2013; Zhang and Chen, 2017), and thus far no study reported conducting a systematic evaluation of the effects of SFD in comparison to other detrending methods, on final chronologies.

3.2. SFD increases agreement at the stand level

In nearly all (more than 90 %), chronologies that had been produced by SFD had higher r-bar values than did those created using traditional detrending methods (Fig. 2). However, for both the PAGES and Missouri networks, the overall improvement was very small: 0.01 in PAGES and 0.02 in the case of MRB (r-bar typically varies between zero and one). For the MRB set, we observed a weak negative relationship between effect size and initial r-bar value, indicating the improvement was greater at lower initial values (Fig. 2, right). There was no apparent relationship between initial value and effect size in the PAGES database (Fig. 3, left). It should be noted that the increase in r-bar was not universal, and there were a few chronologies in each network that experienced a decrease in r-bar due to the signal-free procedure (19 of 298 for PAGES, 7 of 371 or MRB). There was nothing obviously exceptional about these chronologies; all of which spanned at least 250 years with no particular geographic pattern or association with species. Additionally, the sample depth of chronologies that experienced a decrease in r-bar was consistent with the network-wide average, indicating that this negative change was not due to poor replication. The decrease was also very modest, with changes observed only at the hundredth or thousandth decimal place. The application of the signal-free procedure did increase the useful length of final chronologies by pushing the 0.85 EPS cutoff date further into the past. For both networks, SFD extended the average chronology length by approximately a decade (11 years for PAGES to 486 years, 12 years for MRB to 509 years). Results from Wilcox signed-rank tests indicate that the change in rbar following the application of SFD was highly statistically significant (PAGES: $n = 298$, $v = 39970$, $p < 0.001$, MRB: $n = 371$, $v = 68427$, $p < 0.001$).

3.3. SFD increases between-chronology coherence at a regional scale

Scaling up from our analysis of stand-level coherence, we examined the effects of SFD on the strength of correlations between neighboring chronologies. We present the results of this analysis for the original (unsmoothed) versions of each network, and on versions that have been smoothed using low-pass filters set at thirty and one hundred years. Our results were mixed: In the case of PAGES, SFD increased the strength of the correlation between neighbors for the smoothed chronologies (Fig. 3, top panel). However, the opposite was true in the case of MRB. In that case, the unsmoothed traditional version of the network was the most strongly correlated at regional scales and smoothing and SFD decreased the strength of correlation between neighbors (Fig. 3, bottom panel). The results of the Wilcoxon signed-rank tests indicate that the change (increase in PAGES and decrease in MRB) in correlation between neighbors with the application SFD was statistically significant ($p < 0.001$) for the smoothed versions of both networks (Fig. 3, Table S2).

3.4. Variance at medium and low-frequencies greater in SFD chronologies

In order to address the question of whether SFD changes medium- and low-frequency variability in tree-ring chronologies, we examined whether SFD increased spectral power and variance present at decadal and greater timescales across both networks. We observed little to no change at interannual to multi-decadal timescales. However, SFD increase the spectral density at fifty-year and greater wavelengths for both networks, with the greatest change at multi-centennial timescales (between 100–500 years; Fig. 4). This was particularly true for the PAGES network, where the largest difference was at the longest time periods (Fig. 4, top). For MRB, SFD boosted spectral power at fifty-year wavelengths and longer, with the greatest difference at 200−500 years (Fig. 4, bottom). We truncated the spectral plot at 500 years because we had very few chronologies that were long enough to resolve changes at greater than 500 years.

We then smoothed the chronologies with cubic splines at four different wavelengths and calculated the difference in variance between the traditional and signal-free versions. We found that SFD increased the amount of variance at medium-frequencies in PAGES but not MRB chronologies (Fig. 5). In PAGES, we observed an increase in the percent variance of between 5% and 15 % on average, with the largest difference at centennial timescales (Fig. 5, top right). For the MRB network, we similarly observed a 5–10% increase (on average) in the percentage of variance retained at medium frequencies, with the greatest difference at multi-decadal timescales. (Fig. 5, bottom).

Finally, we examined the year-by-year differences in ring-width indices across the PAGES network to examine the effects of SFD on the expression of long-term climate fluctuations (Fig. 6). We averaged across years for all chronologies present in the network, and then took the difference between the traditional and signal-free versions of each chronology. Chronology variance appeared to decrease with sample density, but overall the difference between the traditional and signal-free versions of the chronology was very slight (mean of the absolute value of the difference in RWI of 0.02). In general, SFD increased the recent growth trends across the PAGES network during the second half of the twentieth century (Fig. 6, top panel). This modern increase could be the result of the SFD procedure retaining a signal related to warming

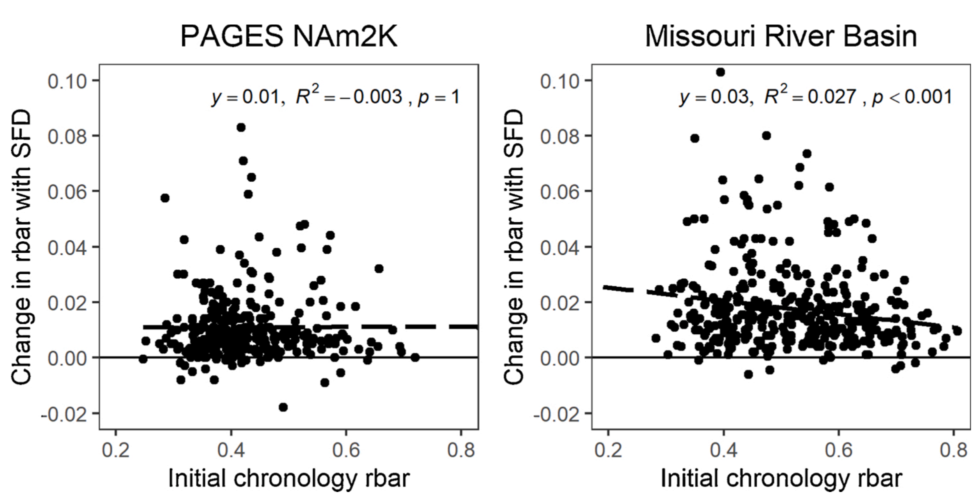

Fig. 2. Change in chronology r-bar values with signal-free procedure. Trend line represents the linear relationship between the r-bar of the traditional version and change with SFD.

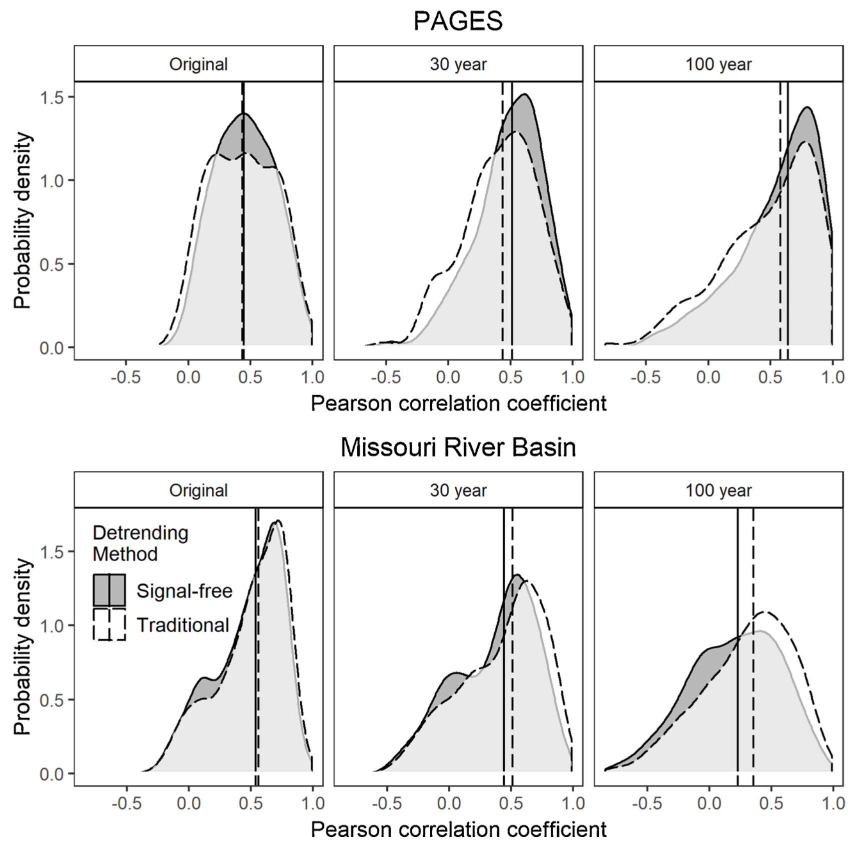

Fig. 3. Pearson correlations between neighboring (sites less than 25 km apart) chronologies for the original and smoothed versions of each chronology pair. Distributions are shown here fitted with probability density functions. Vertical lines represent the median of the distribution. Sample size was 298 in PAGES and 371 in MRB, results of the Wilconxon signed-rank tests for change in in correlation were highly significant ($p < 0.001$) for all smoothed chronology comparisons.

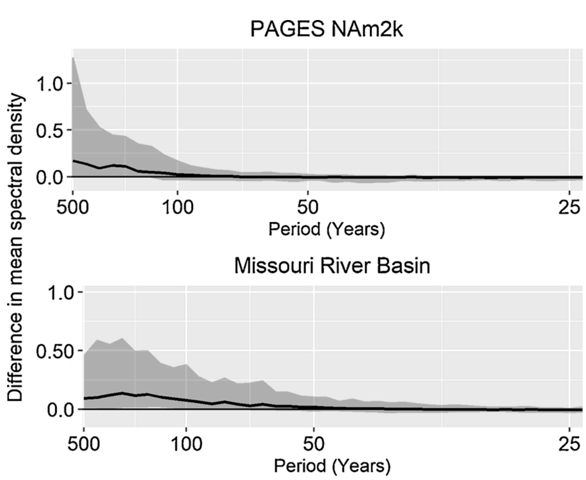

Fig. 4. Impact of signal-free detrending on the spectral structure of chronologies in the PAGES and Missouri tree-ring networks. We differenced the power spectrum for each chronology pair (generated using signal-free and traditional detrending methods) and computed the median change (thick black line) and 5th and 95th percentiles (gray shading) across both networks. Positive values indicate that the signal-free version of the chronology had more variance at a given period than its traditional counterpart, while negative values show the opposite change.

temperatures, but could also represent the amplification of that same trend beyond what would be expected due to warming.

4. Discussion

4.1. *Effects of SFD on coherence across spatial scales*

Signal-free detrending has been widely adopted by dendrochronologists as a data-processing technique intended to improve common signal quality, increase the retention of medium-frequency variability, and avoid non-climatic end effects in tree-ring chronologies. Here we tested whether SFD (i) increases common signal from the stand-level to the regional scale, and (ii) preserves medium-to-low frequency variability. We found that, while on average across the networks SFD increased the expression of medium-frequency variability, it did not universally improve chronology coherence, particularly on a regional scale. Our results underscore the importance of comparing different detrending choices as a step in the process of developing tree-ring chronologies for use in climate reconstructions, and the value of explicitly reporting the results of those tests in publications. While assumptions made about the impacts of SFD on individual chronologies are generally supported by our results, on a regional basis it did not universally improve chronology coherence. We caution that applying SFD across large tree ring networks may even cause regional common signals to weaken.

At the stand-level, we found that SFD marginally improved chronology r-bar values in the large majority of cases for both temperature and moisture sensitive records. It also slightly increased the usable length of the chronologies by an average of a decade in both networks. However, because the SFD process amplifies any stand-wide growth pattern an increase in r-bar cannot necessarily be attributed to climate.

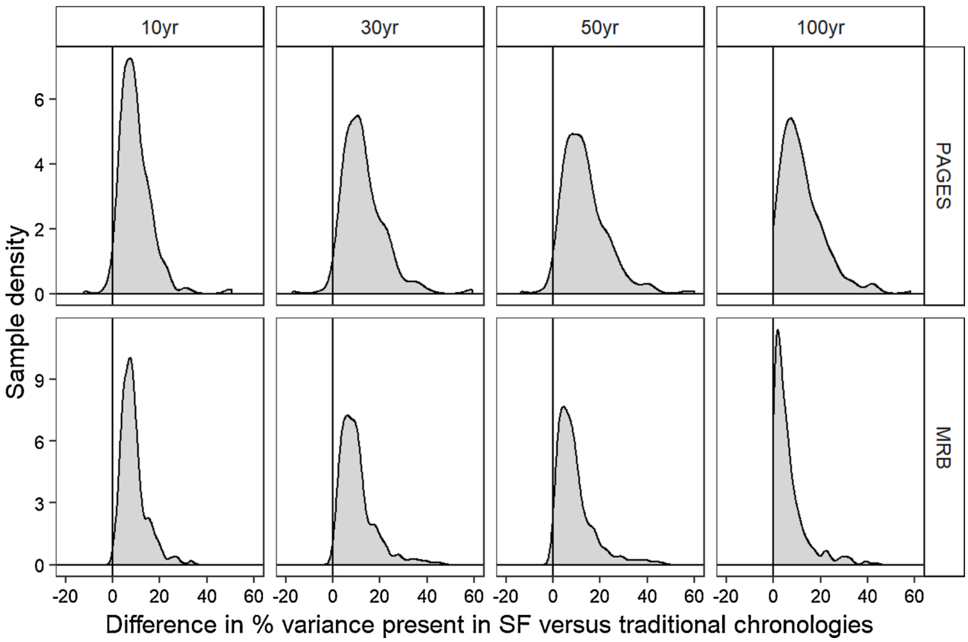

Fig. 5. Relative change in the percent variance retained after smoothing with low-pass filters by applying a 10-yr, 30-yr, 50-yr, or 100-yr spline in signal-free chronologies compared to their traditional chronology counterparts. Percentages greater than zero (less than zero) indicate cases where the signal-free procedure generated a chronology with more (less) variance at the specified wavelengths than the traditional chronology. Vertical bars represent zero, or no change from traditional to SFD chronologies.

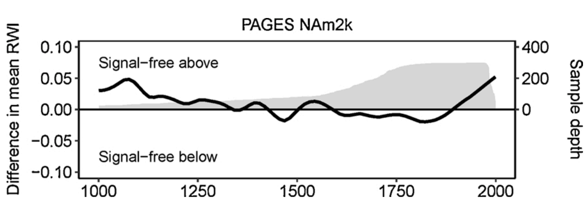

Fig. 6. Difference in mean RWI across the PAGES tree ring network for the last millennia, and sample density at each year represented. "Signal-free above" (below) indicates that SFD resulted in an increase (decrease) in the mean RWI across the network for that year. Sample depth refers to the number of chronologies contributing to the analysis at that year.

Climate signals in tree rings are spatially extensive but stand-wide disturbances by wind (Veblen et al., 1989), insect defoliation (Leland et al., 2016; Clark et al., 2017), or other factors such as demographic recruitment pulses that influence a significant number of trees will also emerge as common signals. Our analysis of neighboring chronologies in which SFD only improved coherence in some records (PAGES) but not others (MRB) would suggest that, although site-level coherence is improving, those effects may not always reflect a climate signal, which would be expected to be similar within a twenty-five kilometer radius.

We predicted that SFD would increase coherence at the regional scale by increasing the correlation strength of neighboring chronologies. Although factors such as altitude, landscape position, and exposure might result in differences in temperature and hydroclimate at a microscale for some pairs, across both networks we predicted at least a slight increase in correlation resulting from SFD within twenty-five kilometers. In the original (unsmoothed) versions of both networks, we found no change in regional correlation strength. However, we did see a change in both networks after we applied low-pass filters at ten and thirty-year wavelengths. In the case of PAGES, we found an increase in correlation strength with SFD, indicating that SFD increased the similarity of neighboring chronologies. However, the opposite was true in the case of MRB, where we observed a decrease in correlation strength with SFD at lower frequencies. This finding may also indicate that the SFD process can sometimes introduce a unique medium- to low-frequency noise component into the final chronologies (e.g., Pearl et al., 2017), making them less similar at regional scales. It is also possible that, rather than amplifying regional climate signals, SFD has increased the expression of stand-wide disturbance events or unique microsite conditions resulting in a degradation of common signals at regional scales. This finding has implications for tree-ring network development – in some cases SFD may decrease the strength of regional patterns by introducing medium-frequency noise or boosting divergent environmental signals.

4.2. Medium- and low-frequency variability and regional coherence

Our analysis of medium- and low-frequency variability retention gives additional insight into the divergent behavior in regional coherence between the two networks. In the case of both PAGES and MRB we saw an increase in medium-frequency variability and low-frequency spectral density in the signal-free chronologies at multi-decadal and greater timescales. The signal-free versions of the PAGES chronologies retained the greatest amount of medium-frequency variability compared with the traditional versions. This shift may explain the increase in correlation strength between neighbors, which was greatest in the low-pass filtered PAGES chronologies. Taken together, these changes suggest the signal-free procedure is increasing the strength of decadal to centennial-scale common signals and that this pattern is spatially coherent, which is to be expected. Conversely, in the case of the MRB chronologies, we observed that SFD was making neighboring sites becoming more dissimilar, despite an increase in medium-frequency variability. This is possibly because MRB chronologies are sensitive to a greater variety of climate signals (Martin et al., 2019). Because the MRB chronologies are selected to reflect the varying components of runoff, this network includes chronologies that are sensitive to a mix of cool-season snowpack, summer precipitation, and warm season temperature. The multi-variate climate signals contained within the MRB database may also help explain the divergent behavior of neighboring chronologies when the SFD procedure was applied. While our findings imply that SFD does generally amplify the medium-frequency component of tree-ring chronologies, that enhancement does not always translate into a concomitant increase in the strength of regional-scale common patterns.

4.3. Limitations and future questions

We tested the claim that SFD increases common signal and improves the retention of medium- to low-frequency variability in tree-ring chronologies. In our review of the literature, these were two of the most commonly stated reasons for applying this method. However, the most cited reason for using SFD in chronology development was in order to reduce trend distortion – an issue that we did not address in this study. Trend distortion occurs when the climate growth relationship becomes either erroneously inflated or suppressed during detrending, resulting in a divergence between climate records and ring-width indices (Cook and Peters, 1997; Melvin and Briffa, 2008). The question of whether or not SFD reduces bias cannot be answered by examining the tree-ring chronologies alone, as it is impossible to know precisely to what degree trends are climate-related (or related to other non-climatic environmental factors), and which are the result of data processing. For example, we observed that SFD increased the magnitude of the presumptive warming trend in the PAGES network (Fig. 6, top panel). Many temperature reconstructions have struggled to capture the magnitude of the recent warming trend observed in instrumental records (D'Arrigo et al., 2006; Wilson et al., 2007; D'Arrigo et al., 2008). This phenomenon, termed the `divergence problem' in which tree rings appear to be losing sensitivity to recent climate warming, was posited by Melvin and Briffa (2008) to result in some cases from the distortion of decadal-scale trends when detrending using traditional approaches. A majority of authors in our literature review also cited reducing trend distortion as their motivation for using SFD. Thus, researchers may determine that the increase in recent growth trends that we observe here accurately reflects the response of trees to anthropogenic climate change. However, we caution that there is also evidence that a subtle growth trend can be inflated though the iterative SFD procedure (c.f. Pearl et al., 2017). Simulating a set of tree-ring series using climate inputs with known variance at particular frequencies could be one method to test the performance of SFD as a means to reduce end effects (Bunn et al., 2004; Vaganov et al., 2011; Anchukaitis et al., 2013; D'Arrigo et al., 2012).

Declaration of Competing Interest

The authors declare that they have no known competing financial interests or personal relationships that could have appeared to influence the work reported in this paper.

Acknowledgements

We thank Dr. Nick McKay at Northern Arizona University for access to the PAGES database. We would also like to thank Drs. Dan Griffin, Toby Ault, and Kurt Kipfmueller for their input and ideas on this topic. This research was funded under National Science Foundation grant number 16025212: Quantifying the risk of widespread megadrought in North America. K.J.A acknowledges support from NSF Division of Atmospheric and Geospace Sciences 1304262 and Division of Atmospheric and Geospace Sciences 1803995. Funding to compile the PAGES NAm2 K dataset was provided by the USGS Powell Center for Synthesis and Analysis. Additional funding for M.Y.M was provided by the University of Minnesota Department of Geography, Environment & Society. This paper is a contribution to the PAGES 2k Network, a working group of the Past Global Changes (PAGES) project that is funded by the Swiss Academy of Sciences and the Chinese Academy of Sciences. Any use of trade, firm, or product names is for descriptive purposes only and does not imply endorsement by the U.S. Government.

Appendix A. Supplementary data

Supplementary material related to this article can be found, in the online version, at doi:https://doi.org/10.1016/j.dendro.2020.125755.

References

Allen, K.J., Drew, D.M., Downes, G.M., Evans, R., Cook, E.R., Battaglia, M., Baker, P.J., 2013. A strong regional temperature signal in low-elevation Huon pine. J. Quaternary Sci. 28, 433–438. https://doi.org/10.1002/jqs.2637.

Allen, K.J., Nichols, S.C., Evans, R., Cook, E.R., Allie, S., Carson, G., Ling, F., Baker, P.J., 2015. Preliminary December–January inflow and streamflow reconstructions from tree rings for western Tasmania, southeastern Australia. Water Resour. Res. 51, 5487–5503. https://doi.org/10.1002/2015WR017062.

Allen, K.J., Fenwick, P., Palmer, J.G., Nichols, S.C., Cook, E.R., Buckley, B.M., Baker, P. J., 2017a. A 1700-year athrotaxis selaginoides tree-ring width chronology from southeastern Australia. Dendrochronologia 45, 90–100. https://doi.org/10.1016/j.dendro.2017.07.004.

Allen, K.J., Nichols, S.C., Evans, R., Allie, S., Carson, G., Ling, F., Cook, E.r., Lee, G., Baker, P.J., 2017b. A 277 year cool season dam inflow reconstruction for Tasmania, southeastern Australia. Water Resour. Res. 53, 400–414. https://doi.org/10.1002/2016WR018906.

Anchukaitis, K.J., D'Arrigo, R.D., Andreu-Hayles, L., Frank, D., Verstege, A., Curtis, A., Buckley, B.M., Jacoby, G.C., Cook, E.R., 2013. Tree-ring-Reconstructed summer temperatures from Northwestern North America during the last nine centuries. J. Climate 26, 3001–3012. https://doi.org/10.1175/JCLI-D-11-00139.1.

Briffa, K.R., Melvin, T.M., 2011. A Closer Look at Regional Curve Standardization of Tree-Ring Records: Justification of the Need, a Warning of Some Pitfalls, and Suggested Improvements in Its Application, in: Dendroclimatology, Developments in Paleoenvironmental Research. Springer, Dordrecht, pp. 113–145. https://doi.org/10.1007/978-1-4020-5725-0_5.

Briffa, K.R., Jones, P.D., Schweingruber, F.H., Karlén, W., Shiyatov, S.G., 1996. Tree-ring variables as proxy-climate indicators: problems with low-frequency signals. In: Jones, P.D., Bradley, R.S., Jouzel, J. (Eds.), Climatic Variations and Forcing Mechanisms of the Last 2000 Years, NATO ASI Series. Springer, Berlin Heidelberg, pp. 9–41.

Briffa, K.R., Osborn, T.J., Schweingruber, F.H., Harris, I.C., Jones, P.D., Shiyatov, S.G., Vaganov, E.A., 2001. Low-frequency temperature variations from a northern tree ring density network. J. Geophys. Res. Atmos. 106, 2929–2941. https://doi.org/10.1029/2000JD900617.

Bunn, A.G., Sharac, T.J., Graumlich, L.J., 2004. Using a simulation model to compare methods of tree-ring detrending and to investigate the detectability of low-frequency signals. Tree Ring Res. 60, 77–90. https://doi.org/10.3959/1536-1098-60.2.77.

Cahoon, S.M.P., Sullivan, P.F., Brownlee, A.H., Pattison, R.R., Andersen, H.-E., Legner, K., Hollingsworth, T.N., 2018. Contrasting drivers and trends of coniferous and deciduous tree growth in interior Alaska. Ecology 99, 1284–1295. https://doi.org/10.1002/ecy.2223.

Cerrato, R., Salvatore, M.C., Gunnarson, B.E., Linderholm, H.W., Carturan, L., Brunetti, M., De Blasi, F., Baroni, C., 2019. A Pinus cembra L. tree-ring record for late spring to late summer temperature in the Rhaetian Alps, Italy. Dendrochronologia 53, 22–31. https://doi.org/10.1016/j.dendro.2018.10.010.

Clackett, S.P., Porter, T.J., Lehnherr, I., 2018. 400-Year record of atmospheric mercury from tree-rings in Northwestern Canada. Environ. Sci. Technol. 52, 9625–9633. https://doi.org/10.1021/acs.est.8b01824.

Clark, P.W., Speer, J.H., Winship, L.J., 2017. Identifying and separating Pandora moth Outbreaks and climate from a 1500-year ponderosa pine chronology from central Oregon. BioOne 73, 113–125. https://doi.org/10.3959/1536-1098-73.2.113.

Cook, E.R., 1987. The Decomposition of Tree-ring Series for Environmental Studies. Tree-ring bulletin, USA.

Cook, E.R., Kairiukstis, L.A., 1990. Methods of Dendrochronology: Applications in the Environmental Sciences. Springer Science & Business Media.

Cook, E.R., Peters, K., 1997. Calculating unbiased tree-ring indices for the study of climatic and environmental change. Holocene 7, 361–370. https://doi.org/10.1177/095968369700700314.

Cook, E.R., Briffa, K.R., Meko, D.M., Graybill, D.A., Funkhouser, G., 1995. The "segment length curse" in long tree-ring chronology development for palaeoclimatic studies. Holocene 5, 229–237. https://doi.org/10.1177/095968369500500211.

Cook, E.R., Seager, R., Cane, M.A., Stahle, D.W., 2007. North American drought: reconstructions, causes, and consequences. Earth. Rev. 81, 93–134. https://doi.org/10.1016/j.earscirev.2006.12.002.

Cook, E.R., Palmer, J.G., Ahmed, M., Woodhouse, C.A., Fenwick, P., Zafar, M.U., Wahab, M., Khan, N., 2013. Five centuries of Upper Indus River flow from tree rings. J. Hydrol. 486, 365–375. https://doi.org/10.1016/j.jhydrol.2013.02.004.

Cook, B.I., Williams, A.P., Smerdon, J.E., Palmer, J.G., Cook, E.R., Stahle, D.W., Coats, S., 2018. Cold tropical pacific sea surface temperatures during the late sixteenth-century north american megadrought. J. Geophys. Res. Atmos. 123 (11), 307–311. https://doi.org/10.1029/2018JD029323, 320.

Cook, E.R., et al., 2020. Old World megadroughts and pluvials during the Common Era. Sci. Adv. 1, e1500561 https://doi.org/10.1126/sciadv.1500561.

D'Arrigo, R., Wilson, R., Jacoby, G., 2006. On the long-term context for late twentieth century warming. J. Geophys. Res. Atmos. 111 https://doi.org/10.1029/2005JD006352.

D'Arrigo, R., Wilson, R., Liepert, B., Cherubini, P., 2008. On the 'Divergence Problem' in Northern Forests: a review of the tree-ring evidence and possible causes. Glob. Planet. Change 60, 289–305. https://doi.org/10.1016/j.gloplacha.2007.03.004.

D'Arrigo, R., Anchukaitis, K.J., Buckley, B., Cook, E., Wilson, R., 2012. Regional climatic and North Atlantic Oscillation signatures in West Virginia red cedar over the past millennium. Glob. Planetary Change Perspect. Clim. Medieval Time 84–85, 8–13. https://doi.org/10.1016/j.gloplacha.2011.07.003.

Deng, Y., Gou, X., Gao, L., Yang, T., Yang, M., 2014. Early-summer temperature variations over the past 563yr inferred from tree rings in the Shaluli Mountains,

southeastern Tibet Plateau. Quat. Res. 81, 513–519. https://doi.org/10.1016/j.yqres.2013.08.002.
Drew, D.M., Allen, K., Downes, G.M., Evans, R., Battaglia, M., Baker, P., 2013. Wood properties in a long-lived conifer reveal strong climate signals where ring-width series do not. Tree Physiol. 33, 37–47. https://doi.org/10.1093/treephys/tps111.
Esper, J., Cook, E.R., Schweingruber, F.H., 2002. Low-frequency signals in long tree-ring chronologies for reconstructing past temperature variability. Science 295, 2250–2253. https://doi.org/10.1126/science.1066208.
Esper, J., Cook, E.R., Krusic, P.J., Peters, K., Schweingruber, F.H., 2003. Tests of the RCS Method for Preserving Low-Frequency Variability in Long Tree-Ring Chronologies. Tree-Ring Research.
Friedman, J.H., 1984. A Variable Span Smoother. Technical Report 5, Laboratory for Computational Statistics Department of Statistics. Stanford University, California.
Fritts, H., 1976. Tree Rings and Climate. Elsevier.
Fuentes, Mauricio, Salo, Riikka, Björklund, Jesper, Seftigen, Kristina, Zhang, Peng, Gunnarson, Björn, Aravena, Juan-Carlos, Linderholm, Hans W., 2017. A 970-year-long summer temperature reconstruction from Rogen, west-central Sweden, based on blue intensity from tree rings. Holocene, 0959683617721322. https://doi.org/10.1177/0959683617721322.
Fuentes, M., Aravena, J.C., Seim, A., Linderholm, H.W., 2019. Assessing the dendroclimatic potential of Nothofagus betuloides (Magellan's beech) forests in the southernmost Chilean Patagonia. Trees 33, 557–575. https://doi.org/10.1007/s00468-018-1801-1.
Gotelli, N.J., Ellison, A.M., 2013. A Primer of Ecological Statistics. Sinauer.
Helama, S., Lindholm, M., Timonen, M., Eronen, M., 2004. Detection of climate signal in dendrochronological data analysis: a comparison of tree-ring standardization methods. Theor. Appl. Climatol. 79, 239–254. https://doi.org/10.1007/s00704-004-0077-0.
Helama, S., Melvin, T.M., Briffa, K.R., 2017. Regional curve standardization: state of the art. Holocene 27, 172–177. https://doi.org/10.1177/0959683616652709.
Helama, S., Arppe, L., Timonen, M., Mielikäinen, K., Oinonen, M., 2018. A 7.5 ka chronology of stable carbon isotopes from tree rings with implications for their use in palaeo-cloud reconstruction. Glob. Planet. Change 170, 20–33. https://doi.org/10.1016/j.gloplacha.2018.08.002.
Leland, C., Hom, J., Skowronski, N., Ledig, F.T., Krusic, P.J., Cook, E.R., Martin-Benito, D., Martin-Fernandez, J., Pederson, N., 2016. Missing rings, synchronous growth, and ecological disturbance in a 36-Year pitch pine (Pinus rigida) provenance study. PLoS One 11, e0154730. https://doi.org/10.1371/journal.pone.0154730.
Martin, J.T., Pederson, G.T., Woodhouse, C.A., Cook, E.R., McCabe, G.J., Wise, E.K., Erger, P., Dolan, L., McGuire, M., Gangopadhyay, S., Chase, K., Littell, J.S., Gray, S T., George, S.St., Friedman, J., Sauchyn, D., Jacques, J.St., King, J., 2019. 1200 years of Upper Missouri River streamflow reconstructed from tree rings. Quat. Sci. Rev. 224, 105971 https://doi.org/10.1016/j.quascirev.2019.105971.
Maxwell, R.s., Harley, G.l., Maxwell, J.t., Rayback, S.a., Pederson, N., Cook, E.r., Barclay, D.j., Li, W., Rayburn, J.a., 2017. An interbasin comparison of tree-ring reconstructed streamflow in the eastern United States. Hydrol. Process. 31, 2381–2394. https://doi.org/10.1002/hyp.11188.
Melvin, T., 2004. Historical Growth Rates and Changing Climatic Sensitivity of Boreal Conifers. University of East Anglia.
Melvin, T.M., Briffa, K.R., 2008. A "signal-free" approach to dendroclimatic standardisation. Dendrochronologia 26, 71–86. https://doi.org/10.1016/j.dendro.2007.12.001.
Melvin, T.M., Briffa, K.R., 2014a. CRUST: software for the implementation of regional chronology standardisation: part 1. Signal-Free RCS. Dendrochronol. 32, 7–20. https://doi.org/10.1016/j.dendro.2013.06.002.
Melvin, T.M., Briffa, K.R., 2014b. CRUST: software for the implementation of regional chronology standardisation: part 2. Further RCS options and recommendations. Dendrochronologia 32, 343–356. https://doi.org/10.1016/j.dendro.2014.07.008.
PAGES 2k Consortium, 2013. Continental-scale temperature variability during the past two millennia. Nat. Geosci. 6, 339–346. https://doi.org/10.1038/ngeo1797.
PAGES2k Consortium, 2017. A global multiproxy database for temperature reconstructions of the Common Era. Sci. Data 4, 170088. https://doi.org/10.1038/sdata.2017.88.
Palmer, J.G., Cook, E.R., Turney, C.S.M., Allen, K., Fenwick, P., Cook, B.I., O'Donnell, Alison, Lough, J., Grierson, P., Baker, P., 2015. Drought variability in the eastern Australia and New Zealand summer drought atlas (ANZDA, CE 1500–2012) modulated by the Interdecadal Pacific Oscillation. Environ. Res. Lett. 10, 124002 https://doi.org/10.1088/1748-9326/10/12/124002.
Pearl, J.K., Anchukaitis, K.J., Pederson, N., Donnelly, J.P., 2017. Reconstructing Northeastern United States temperatures using Atlantic white cedar tree rings. Environ. Res. Lett. 12, 114012 https://doi.org/10.1088/1748-9326/aa8f1b.
Pederson, G.T., Gray, S.T., Woodhouse, C.A., Betancourt, J.L., Fagre, D.B., Littell, J.S., Watson, E., Luckman, B.H., Graumlich, L.J., 2011. The unusual nature of recent snowpack declines in the North American Cordillera. Science 333, 332–335. https://doi.org/10.1126/science.1201570.
Pederson, N., Tackett, K., McEwan, R.W., Clark, S., Cooper, A., Brosi, G., Eaton, R., Stockwell, R.D., 2012. Long-term drought sensitivity of trees in second-growth forests in a humid region. Can. J. For. Res. 42, 1837–1850. https://doi.org/10.1139/x2012-130.
Priestley, M.B., 1981. Spectral Analysis and Time Series, Probability and Mathematical Statistics. Academic Press, London; New York.
R Core Team, 2019. R: a Language and Environment for Statistical Computing. R Foundation for Statistical Computing, Vienna, Austria.
Shumway, R.H., Stoffer, D.S., 2017. Time Series Analysis and Its Applications: With R Examples. Springer.
Stahle, D.W., Cook, E.R., Burnette, D.J., Villanueva, J., Cerano, J., Burns, J.N., Griffin, D., Cook, B.I., Acuña, R., Torbenson, M.C.A., Szejner, P., Howard, I.M., 2016. The Mexican Drought Atlas: tree-ring reconstructions of the soil moisture balance during the late pre-Hispanic, colonial, and modern eras. Quat. Sci. Rev. 149, 34–60. https://doi.org/10.1016/j.quascirev.2016.06.018.
Vaganov, E.A., Anchukaitis, K.J., Evans, M.N., 2011. How Well understood are the processes that create dendroclimatic records? A mechanistic model of the climatic control on conifer tree-ring growth dynamics. In: Hughes, M.K., Swetnam, T.W., Diaz, H.F. (Eds.), Dendroclimatology: Progress and Prospects, Developments in Paleoenvironmental Research. Springer Netherlands, Dordrecht, pp. 37–75. https://doi.org/10.1007/978-1-4020-5725-0_3.
Veblen, T.T., Hadley, K.S., Reid, M.S., Rebertus, A.J., 1989. Blowdown and stand development in a Colorado subalpine forest. Can. J. For. Res. 19, 1218–1225. https://doi.org/10.1139/x89-186.
Wang, B., Chen, T., Xu, G., Wu, M., Zhang, G., Li, C., Wu, G., 2018. Anthropogenic-management could mitigate declines in growth and survival of Qinghai spruce (Picea crassifolia) in the east Qilian Mountains, northeast Tibetan Plateau. Agric. For. Meteorol. 250–251, 118–126. https://doi.org/10.1016/j.agrformet.2017.12.249.
Wang, X., Pederson, N., Chen, Z., Lawton, K., Zhu, C., Han, S., 2019. Recent rising temperatures drive younger and southern Korean pine growth decline. Sci. Total Environ. 649, 1105–1116. https://doi.org/10.1016/j.scitotenv.2018.08.393.
Wigley, T.M.L., Briffa, K.R., Jones, P.D., 1984. On the average value of correlated time series, with applications in Dendroclimatology and hydrometeorology. J. Climate Appl. Meteor. 23, 201–213. https://doi.org/10.1175/1520-0450(1984)023<0201:OTAVOC>2.0.CO;2.
Wilson, R., D'Arrigo, R., Buckley, B., Büntgen, U., Esper, J., Frank, D., Luckman, B., Payette, S., Vose, R., Youngblut, D., 2007. A matter of divergence: tracking recent warming at hemispheric scales using tree ring data. J. Geophys. Res. Atmos. 112 https://doi.org/10.1029/2006JD008318.
Wise, E.K., 2010. Tree ring record of streamflow and drought in the upper Snake River. Water Resour. Res. 46 https://doi.org/10.1029/2010WR009282.
Woodhouse, C.A., Lukas, J.J., 2006. Drought, tree rings and water resource management in Colorado. Can. Water Resour. J. 31, 297–310. https://doi.org/10.4296/cwrj3104297.
Zhang, X., Chen, Z., 2017. A new method to remove the tree growth trend based on ensemble empirical mode decomposition. Trees 31, 405–413. https://doi.org/10.1007/s00468-015-1295-z.